物 理 化 学 学 报

Acta Phys. -Chim. Sin. **2021,** *37* (9), 2009035 (1 of 15)

[Review] doi: 10.3866/PKU.WHXB202009035 www.whxb.pku.edu.cn

Synthesis and Application of Platinum-Based Hollow Nanoframes for Direct Alcohol Fuel Cells

Lei Huang, Shahid Zaman, Zhitong Wang, Huiting Niu, Bo You, Bao Yu Xia *

Key Laboratory of Material Chemistry for Energy Conversion and Storage (Ministry of Education), Key Laboratory of Material Chemistry and Service Failure, Wuhan National Laboratory for Optoelectronics, School of Chemistry and Chemical Engineering, Huazhong University of Science and Technology, Wuhan 430074, China.

Abstract: Although platinum (Pt)-based catalysts are suffering from high costs and limited reserves, they are still irreplaceable in a short period of time in terms of catalytic performance. Structural optimization, composition regulation and carrier modification are the common strategies to improve the activity and stability of Pt-based catalyst. Strikingly, the morphological evolution of Pt-based electrocatalyst into nanoframes (NFs) have attracted wide attention to reduce the Pt consumption and improve the electrocatalytic activity simultaneously. Contrary to Pt-based solid nanocrystalline materials, Pt-based NFs have many advantages in higher atomic utilization, open space structure and larger specific surface area, which facilitate electron transfer, mass transport and weaken surface adsorption by more unsaturated coordination sites. Here we introduce the detailed preparation strategies of Pt-based NFs with different etching methods (oxidative etching, chemical etching, galvanic replacement and carbon monoxide etching), crystal structure evolution and formation mechanism, efficient applications for oxygen reduction reaction (ORR), methanol oxidation reaction (MOR) and ethanol oxidation reaction (EOR) in direct alcohol fuel cells (DAFCs). Based on the high-efficiency atom utilization, open space structure and diverse alloy composition, Pt-based NFs exhibit superior activity, stability and anti-poisoning than commercial counterparts in the application of DAFCs. The current challenges and future development of Pt-based NFs are prospected on the type of NFs materials, synthesis and etching methods, crystal control and catalytic performance. We propose a series of improvement mechanisms of Pt-based NFs, such as small size effect, high-energy facets, Pt-skin construction and Pt-C integration, thereby weakening the molecule absorption, increasing the Pt utilization, strengthening the intrinsic stability, and alleviating the metal dissolution and support corrosion. Additionally, the scale-up synthesis of catalytic materials, membrane electrodes assembly, and development of the start-stop system and the circulation system design are essential for the commercial application of Pt-based NFs and industrial manufacturing of DAFCs. More importantly, the reaction mechanism, active site distribution and dynamic changes in the catalytic material during the catalytic reaction are crucial to further explain the maintenance and evolution of catalytic performance, which will open a window to elucidate the improvement mechanism of the catalyst in the fuel cell reactions. This review work would promote continuous upgradations and understandings on Pt-based NFs in the future development of DAFCs.

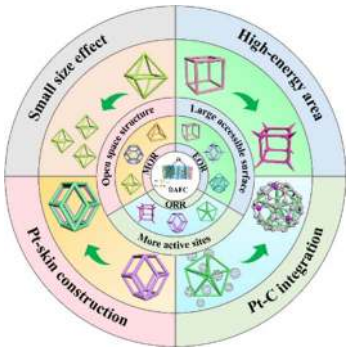

Key Words: Fuel cell; Electrocatalyst; Platinum alloy; Nanoframe; Etching

Received: September 9, 2020; Revised: October 11, 2020; Accepted: October 12, 2020; Published online: October 23, 2020.

*Corresponding author. Email: byxia@hust.edu.cn.

The project was supported by the National Natural Science Foundation of China (22075092), the Program for HUST Academic Frontier Youth Team (2018QYTD15) and the National 1000 Young Talents Program of China.

国家自然科学基金(22075092), 华中科技大学学术前沿青年团队项目(2018QYTD15)和国家青年千人计划资助

铂基空心纳米框架的合成及其在直接醇燃料电池中的应用

黄磊，Shahid Zaman，王志同，牛慧婷，游波，夏宝玉*

华中科技大学化学与化工学院，能量转换与存储材料化学教育部重点实验室，材料化学与服役失效湖北省重点实验室，武汉光电国家研究中心，武汉 430074

摘要：与其他铂基纳米晶体材料相比，铂基纳米框架催化剂因其独特的结构特征和优异的催化性能引起研究者的广泛关注。开放的空间结构设计和组分可控调制不仅提高了铂的原子利用率，而且能在减少铂消耗的同时改善其电催化活性。本文简要综述了铂基纳米框架电催化剂的最新进展。在介绍不同的铂基纳米框架制备和蚀刻策略之后，也对框架晶体的结构演变及其在醇燃料电池中氧还原反应和醇氧化反应的催化应用进行了总结。此外，基于纳米框架材料的类型、合成方法、结构形态和催化性能，对铂基纳米框架的当前存在的挑战和未来的发展前景进行了总结和展望。基于铂基纳米框架材料的改进机制和规模化制备策略，我们相信纳米框架材料将会在醇燃料电池等技术中发挥更大作用。

关键词：燃料电池；电催化剂；铂合金；纳米框架；蚀刻

中图分类号：O646

1 Introduction

Hydrogen-oxygen fuel cells have been developed swiftly due to higher conversion efficiency, clean and environment-friendly products and vast hydrogen sources. However, hydrogen storage, transportation and infrastructure of the hydrogen fueling system with desired safety measures still hinder the extensive application of hydrogen energy. Direct alcohol fuel cells (DAFCs) show prominent advantages over hydrogen-oxygen fuel cells due to the easy storage, transportation and safety of liquid fuels, which are decisive for the commercial application of energy technology.

Platinum (Pt)-based catalysts occupy a vital and irreplaceable position in the energy conversion systems [1–3]. Although Pt raw materials have limited reserves and high cost, it is still considered to be the most promising electrocatalyst for oxygen reduction reaction (ORR), methanol oxidation reaction (MOR) and ethanol oxidation reaction (EOR). However, Pt-based catalysts are suffering from poor stability, limited activity and quick poisoning by reaction intermediates during the electrochemical operations in DAFCs, which is a huge obstacle to full-cell [4–6]. Consequently, the development of low-Pt catalysts with high activity and stability has ushered in extensive researches.

In this regard, numerous efforts are devoted to the structural regulation, alloying and multi-component treatment [7–11]. These strategies can reduce Pt consumption and improve the stability and anti-toxicity of Pt-based catalysts through a series of chain effects (such as stress effect, synergistic effect, optimized electronic structure, *etc.*). Starting with the Pt/C catalyst, the size of Pt nanoparticles is firstly controlled to increase the active area according to the size effect (Scheme 1). Next, the high-index facets of Pt particles are designed to increase the surface free energy and decrease the initial coordination number. Subsequently, a large number of alloy materials are introduced to alleviate the Pt dissolution, so that the catalytic activity and stability are strengthened comprehensively under the stress and synergy effects [12]. However, the current high Pt consumption and resultant catalyst cost are not acceptable for commercial applications. Therefore, the reduced Pt consumption and improved activity could be achieved by enriching the Pt atomic exposure at the interface through core-shell and heterogeneous structures with Pt-rich surfaces. Furthermore, the alloyed hollow frames with highly open structure and large accessible surface are promising to improve the activity and stability and promote mass transport, electron transfer and continuous conversion of DAFCs [13].

Among the different structural and compositional optimization strategies of Pt-based catalysts, the anisotropic

Dr. **Bao Yu Xia** is currently a full professor in the School of Chemistry and Chemical Engineering at Huazhong University of Science and Technology (HUST), China. He received his Ph.D. degree in materials science at Shanghai Jiao Tong University (SJTU) in 2010. He worked at Nanyang Technological University (NTU) from 2011 to 2016. His research involves functional materials in sustainable energy and clean environment technologies including fuel cells, batteries, and electrocatalysis.

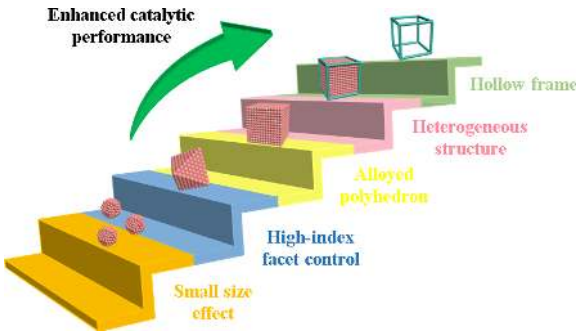

Scheme 1 Development and structural evolution of Pt-based catalysts.

hollow Pt-based nanoframes (NFs) materials attract more extensive attention [14]. Relative to typical Pt/C catalyst, Pt-based NFs materials possess specific advantages of (1) efficient active sites utilization, (2) highly open space structure and larger accessible surface, (3) more unsaturated coordination centers, and (4) enhanced high-energy surface, which can realize the rapid electron transfer and mass transport in the electrocatalytic reaction systems. Additionally, alloy components in the Pt-based NFs can reduce the Pt consumption and catalyst cost along with the induced strain effect, synergistic effect, lattice reconstruction, weakening of adsorption and redesign of Pt electronic structure [15–17]. Therefore, Pt-based alloy NFs can bring advanced physical stability, anti-poisoning capability and catalytic activity.

This review briefly introduces the preparation strategies basis and structural advantages of Pt-based NFs, representative synthetic etching techniques and structural evolution process. Moreover, electrocatalytic applications of Pt-based NFs in ORR, MOR and EOR for DAFCs are highlighted with a focus on the catalytic activity, anti-poisoning ability and durability of Pt-based NFs against Pt/C. More importantly, we discuss the current challenges and future perspectives on Pt-based NFs in practical application of DAFCs, especially the design optimization of catalysts and membrane electrode assembly (MEA) for DAFCs. Also, advanced characterization technology, computational simulation and artificial intelligence will be considered to analyze the catalytic reaction mechanism and structure-activity relationship. We believe this review will stimulate more policymakers and researchers' interest in Pt-based NFs for future energy conversion technology.

2 Formation basis of Pt-based NFs

In general, the formation of Pt-based NFs material is based on solid nanocrystals, which undergoes two basic processes: wet chemical method to synthesize solid polyhedrons, and then remove the internal metal by various etching techniques [18–20]. With the nucleation and growth of Pt nanocrystals, further deposition and outward migration of Pt atoms, a large number of Pt atoms will be eventually deposited on the polyhedron edges [21–23]. Based on the transmission electron microscopic (TEM) images and structural models, the PtCuCo rhombic dodecahedrons possess distinct heterogeneous structures before the etching where most of Pt species are concentrated on the edges and corners of the polyhedrons (Fig. 1a) [24–27]. After the etching treatment, the excess metal on the (110) surface and inner of the crystals is removed, leaving the frame constructed of edges and corners, thereby obtaining Pt alloy NFs. Similarly, PtPd heterogeneous cubes with (100) facets were also converted to PtPd cubic NFs by internal etching (Fig. 1b). Ordered elemental distribution assures the subsequent systematic etching, where a large amount of Pt metal can be retained with etching away of non-Pt metal, leaving only the edges and corners of the polyhedron to form Pt-based NFs. Notably, the formation of

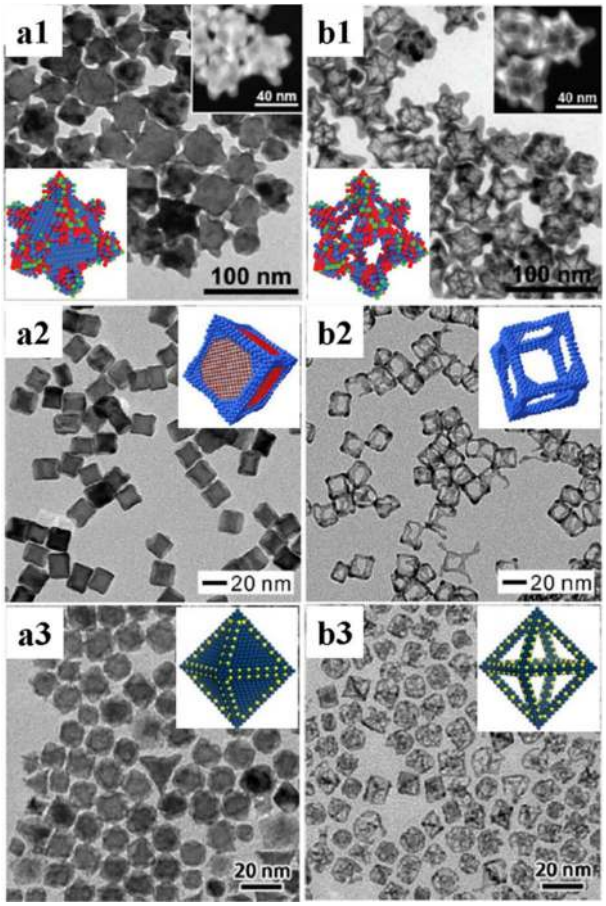

Fig. 1 TEM images of (a) solid polyhedrons, (b) hollow NFs for PtCuCo rhombic dodecahedron, PtPd cube, PtNi octahedra, respectively.

Panels a1, b1 adapted from Ref. 24, copyright 2018 Wiley-VCH. Panels a2, b2 adapted from Ref. 25, copyright 2016 Wiley-VCH. Panels a3, b3 adapted from Ref. 26, copyright 2014 Springer-Verlag.

heterogeneous nanocrystals is an essential prerequisite for the preparation of Pt-based NFs, which provides the possibility for subsequent etching [28]. Likewise, a large amount of Ni metal is corroded from the (111) surface, and finally the PtNi octahedral NFs are obtained. Nowadays, the preparation of Pt-based NFs is mainly based on Pt-based heterostructure nanocrystals, which have a clear trend in element distribution (the corners are dominated by relatively stable Pt metal and the cores and faces are mainly non-platinum metal). Therefore, it could be concluded that a heterogeneous solid polyhedron is essential for the formation of Pt-based NFs. Compared with other Pt-based materials, Pt-based NFs possess irreplaceable advantages: (1) high atomic utilization, (2) open space structure, and (3) large accessible surface [29–31].

3 Structural evolution of Pt-based NFs

According to current reports, the synthesis of Pt-based polyhedral heterogeneous structures is primarily based on wet chemical methods. By selecting appropriate surfactants, reaction solvents and precursors, and adjusting the reaction time and

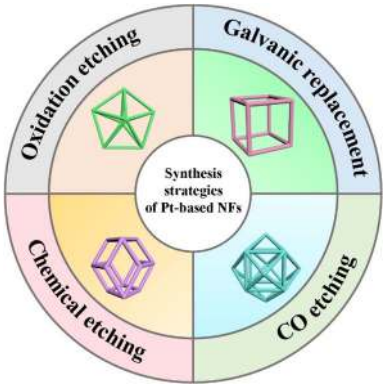

Scheme 2 Schematic diagram of the reported preparation methods of Pt-based NFs.

temperature, the growth and crystallization rate of Pt-based nanocrystals are accurately regulated. Subsequently, different etching strategies are employed to achieve the conversion of solid polyhedrons to NFs. The representative etching methods of Pt-based NFs can be divided into four categories (Scheme 2): (1) oxidative etching, (2) chemical etching, (3) galvanic replacement, and (4) carbon monoxide etching, which collectively constitutes to a complete corrosion system of Pt-based NFs. However, oxidative etching and chemical etching account for a large proportion of these etching techniques of Pt-based NFs (Table 1). Meanwhile, galvanic replacement and carbon monoxide etching have been employed for the preparation of complicated Pt-based NFs. Curiously, some Pt-based NFs are prepared by combining two etching methods. For example, in the preparation of PtCuNi NFs, solid rhombic dodecahedrons are first etched to obtain concave rhombic dodecahedrons, followed by acid etching to collect rhombic dodecahedral PtCuNi NFs [36]. Similarly, the metal Cu and Pd inside the cubic PtPdCu crystal are replaced by an appropriate Fe^{3+} solution, where the internal Pd and Cu metals are dissolved with a small amount of reduced Fe. Subsequently, the remaining metal is etched by adding acid solution to obtain cubic PtPdCu NFs [37]. Therefore, the preparation of Pt-based NFs is not limited to a single etching method, it is flexible and diverse for materials with multiple components and complex structures.

3.1 Oxidative etching

Oxidative etching is one of the most popular etching strategies, especially the synthesis of PtCu-based NFs occupies an absolute predominance [65]. The statistics above further validate the vital role of oxidative etching in the formation of NFs, particularly for the PtCu-based NFs is benefited from the oxidative etching due to the simple operation and excellent structure [35,66]. A series of progressive reports on PtCu-based NFs such as octopod cubic PtCu, concave cubic PtCu, rhombic dodecahedral PtCuNi and rhombic dodecahedral PtCuRh NFs, emphasized the critical role of oxidative etching in the one-step synthesis of PtCu-based NFs [38,40,41]. Under similar conditions, the Pt species are more easily reduced than Cu because the standard redox potential for Cu^{2+} is negative than Pt^{4+}. The structural evolution in the formation of PtCu NFs primarily involves nucleation, growth, overgrowth, and oxidative etching stages (Fig. 2a). In the nucleation stage, thermodynamically stable cubic octahedral crystal nuclei with low-level crystal planes (111) and (100) are preferentially obtained [67–69]. The {100} plane is covered with Br ions in the following growth, leading to the faster deposition rate of metal ions on the corners [70–72]. As a result, the nucleus will selectively and rapidly grow into a concave cube and overgrow in the direction of [111] due to the relatively low residual Pt concentration in the solution. With the formation and selective adsorption of oxidative etching pairs of halide ions (Br^-, Cl^-, I^-) and oxygen, the metal on the {100} facet is removed directionally from the outer to the inner of the crystal to obtain concave cubic PtCu NFs, implying the prominent effect of oxidative etching (Fig. 2b). Likewise, five-fold-twinned and rhombic dodecahedral PtCu NFs are successfully synthesized by selective adsorption of the etching pair followed by oxidative etching (Fig. 2c, d). A clear high-angle annular dark-field scanning transmission electron microscope (HAADF-STEM) observation shows sharp edges and corners, and maintains a complete hollow structure after removing internal metal. These results further demonstrate oxidative etching is an effective strategy for the formation of PtCu-based NFs.

3.2 Chemical etching

Table 1 The reported synthesis methods of Pt-based NFs with various shapes and compositions.

Synthesis method	Shape and composition of Pt-based NFs		
Oxidative etching	Rhombic dodecahedral PtCu [32–35]	Rhombic dodecahedral PtCuNi [36]	Cubic PtPdCu [37]
	Octopod cubic PtCu [38]	Five-Fold-Twinned PtCu [39]	Concave cubic PtCu [40]
	Rhombic dodecahedral PtCuRh [41]	Octahedral PtCu [17,42]	Five-Fold-Twinned PtCuMn [43]
Chemical etching	Rhombic dodecahedral PtNi [44–47]	Vertex-Reinforced PtCuCo [24]	Truncated octahedral PtNiAu [48]
	Spiny rhombic dodecahedral PtCu [49]	Vertex-Reinforced PtCuRh [50]	Octahedral PtNi [26,51]
	Rhombic dodecahedral PtRuNi [52]	Rhombic dodecahedral PtCuNi [36]	Skeletal octahedral PtNi [53]
	Rhombic dodecahedral PtRhNi [54]	Rhombic dodecahedral PtCo [55]	Polyhedral PtCo [56]
	Core-Shell AgAuPt [57]	Truncated octahedral PtAu [58]	PtAu bipyramid [59]
	Ultra-Small PtPdRhAg [60]	Porous Pt-$Bi(OH)_3$ [61]	Dendrite-Embedded PtNi [62]
Galvanic replacement	Cubic PtPdCu [37]	Triangular PtAg [63]	
CO etching	Tetrahexahedral PtNi [64]		

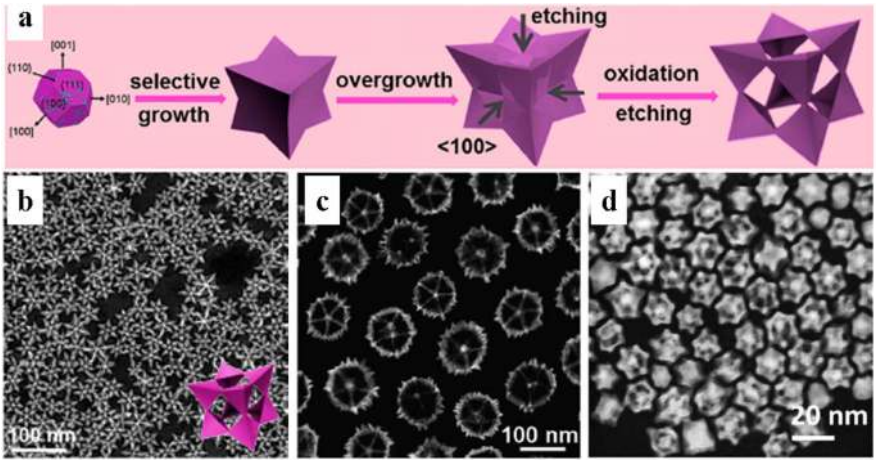

Fig. 2 (a) Schematic of the major steps involved in the formation of concave cubic PtCu NFs. Representative HAADF-STEM images of (b) concave cubic, (c) five-fold-twinned and (d) rhombic dodecahedral PtCu NFs, respectively.

Panels a, b adapted from Ref. 40, copyright 2016 American Chemical Society. Panel c adapted from Ref. 39, copyright 2017 Wiley-VCH. Panel d adapted from Ref. 34, copyright 2018 Wiley-VCH.

Although oxidative etching plays an essential role in the structural evolution of Pt-based NFs, it is less effective for non-PtCu-based and multi-component NFs. Therefore, chemical etching is a more general method for preparing a wide range of Pt-based NFs materials, mainly involves rapid acid etching and slow organic decomposition. The acid etching shows a short experimental cycle and simple operation along with a slow organic decomposition that brings relatively smooth and complete frame morphology. Relative to oxidative etching in one-step preparation, chemical etching usually occurs in the second step after forming solid nanocrystals, which is more flexible in the synthesis of multicomponent Pt-based NFs. The vertex-reinforced PtCuRh NFs are first collected by solvothermal method followed by the etching of metal from interior and surface through a strong acid treatment, leaving the complete crystal frames (Fig. 3a, b) [50]. The active metals are removed during the acid etching where the edges of the polyhedron exhibit strong intrinsic stability due to the Pt enrichment, which allows the frame structure to be maintained under strong corrosion. Also, octahedral PtNi skeleton and rhombic dodecahedral PtNi NFs are synthesized by rapid acid treatment, displaying a highly open structure and complete frames (Fig. 3c, d) [53]. The acid etching method is simple and more profound for the preparation of the various Pt-based alloy NFs, in which the concentration and type of acid can be adjusted to control the corrosion rate and intensity.

Meanwhile, the harsh acid etching may bring structural collapse and damage to the active sites, resulting in rapid degradation of catalytic activity during a long-term durability test. Concerning this issue, a relatively slow and time-consuming organic etching is proposed for the complete hollow Pt-based NFs. A long-period organic etching method is employed to achieve polyhedral PtCo NFs, rhombic dodecahedral PtCo NFs and rhombic dodecahedral PtNi NFs [55,56,73]. The PtNi solid polyhedrons were dispersed in hexane and chloroform, thereby turning into hollow PtNi NFs after two weeks of metal dissolution (Fig. 3e) [45]. Also, the synthesis of octahedra PtNi and truncated octahedral PtNiAu NFs is achieved by organic etching [48]. Although organic etching has extended the corrosion period, the obtained PtNi NFs are more structurally perfect and robust. Contrary to oxidative and acid etching, organic etching consumes more time and cost, yet uniform and perfect NFs can reduce Pt loss and take full advantage of the active sites. As a result, we can consider the most suitable and economical way to prepare different types of Pt-based NFs materials.

3.3 Galvanic replacement

As for some heterogeneous structures with relatively stable internal metals, it is not easy to effectively remove the core metals to get NFs architecture. Therefore, electrochemical replacement is considered to be more effective for the corrosion of these stubborn metals. The classic PtPdCu cubic NFs are fabricated by galvanic replacement, which involves two-step process (Fig. 4a). The first step is to generate cubes with Pd-rich cores and Pt-rich frames serving as the precursor for PtPdCu concave cubes [37]. The cubes with unique heterogeneous structure and elemental distribution are formed through a simple one-pot solvothermal method, which provides an opportunity to synthesize PtPdCu alloy NFs (Fig. 4b). In the successive step, the Pd-rich cores are selectively etched with Fe^{3+}, where Pd cores can be removed to produce PtPdCu alloy NFs (Fig. 4c). Subsequently, excess Fe^{3+} solution is added as an etchant to replace the metal Pd in the etching system, followed by hydrochloric acid addition to remove a small amount of reduced metallic Fe. Finally, the Pd and Cu are completely dissolved to obtain hollow Pt-based NFs (Fig. 4d). Noticeably, the selection of proper etchant is vital by considering the redox potential of the etched metal and added metal ions to remove the reduced metal in the galvanic replacement method.

3.4 Carbon monoxide etching

In addition to common oxidative etching and chemical

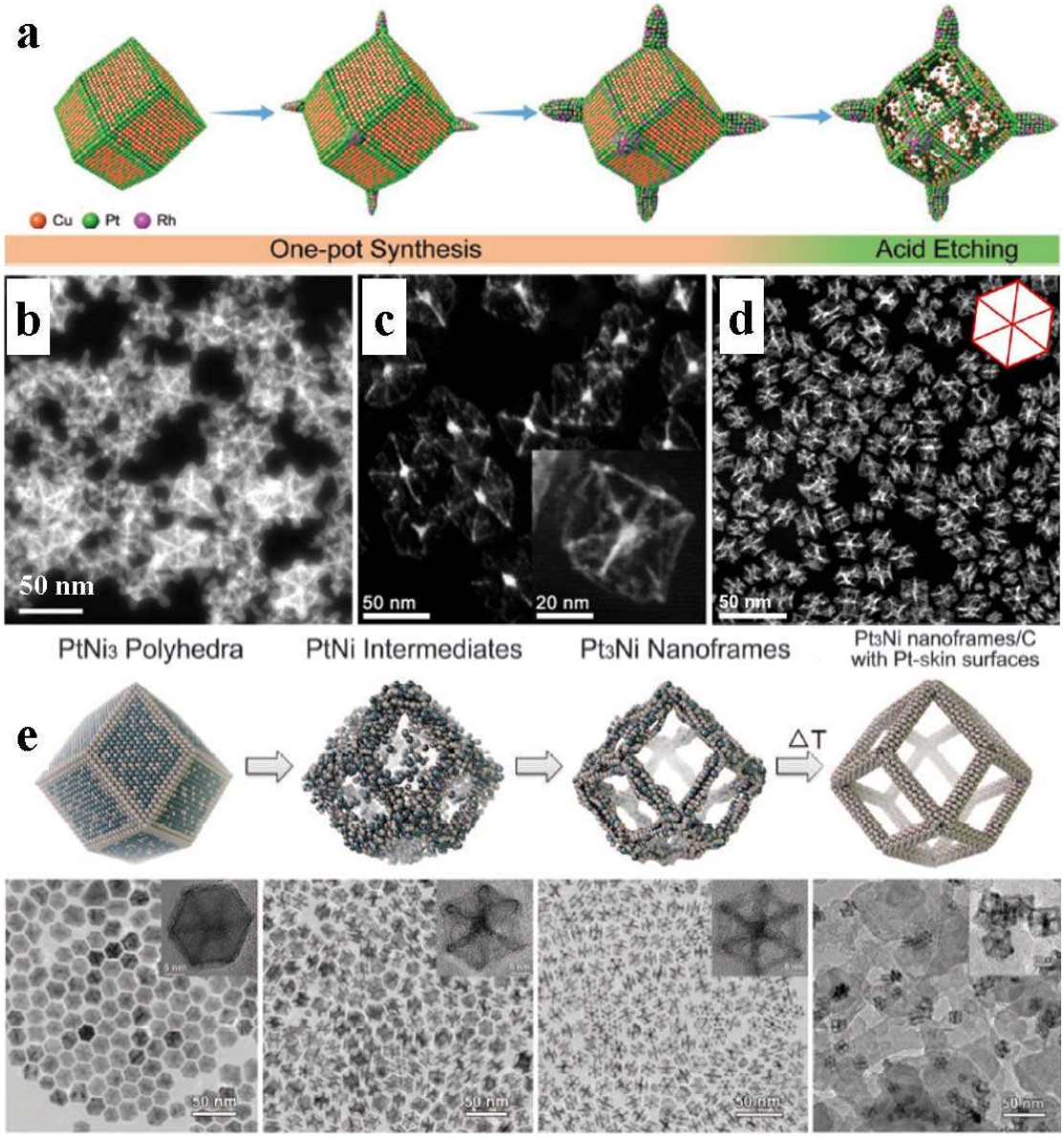

Fig. 3 (a) Preparation process of the vertex-Reinforced PtCuRh NFs; HAADF-STEM images of (b) vertex-reinforced PtCuRh, (c) octahedral PtNi skeleton and (d) rhombic dodecahedral PtNi NFs, respectively; (e) TEM images of initial solid PtNi polyhedrons, PtNi intermediates, hollow PtNi NFs, PtNi NFs with Pt-skin, corresponding schematic illustrations of the samples obtained at four representative stages during the evolution process from polyhedrons to NFs.

Panels a, b adapted from Ref. 50, copyright 2018 Wiley-VCH. Panel c adapted from Ref. 53, copyright 2015 American Chemical Society. Panel d adapted from Ref. 23, copyright 2016 American Chemical Society. Panel e adapted from Ref. 45, copyright 2014 American Association for the Advancement of Science.

corrosion, carbon monoxide etching is rarely reported. Typically, tetrahexahedral PtNi NFs were prepared through the carbon monoxide etching (Fig. 5). Carbon-loaded PtNi nanocrystals were annealed in the presence of carbon monoxide by the Mond process so that Ni was extracted from PtNi nanocrystals to obtain tetrahexahedral PtNi NFs [64]. The selective etching of Ni atoms from the <100> direction is considered as a critical factor that prevents the deformation of PtNi NFs, whereas the internal stress generated during the excavating process is relieved through the thermal annealing and the accompanying surface restructuring [74]. Moreover, the thermal treatment results in segregated Pt alloy with residual Ni atoms, diminishing the uncontrollable vacancy defects and generating stable and well-defined microstructures of a strained Pt thin layer [75]. Therefore, the preparation of Pt-based NFs by carbon monoxide etching faces challenges as well as many opportunities.

Based on the etching of solid polyhedrons, we have carried out an extensive analysis of etching strategies for Pt-based NFs preparation and their applicable scope. Among them, oxidative etching is widely used in the preparation of PtCu-based binary and multivariate NFs. In a solvothermal process, the oxidative etching pairs formed by halide ions and oxygen are used to remove the internal metal of solid polyhedrons in a single step. Although the oxidative etching is simple in operation and more

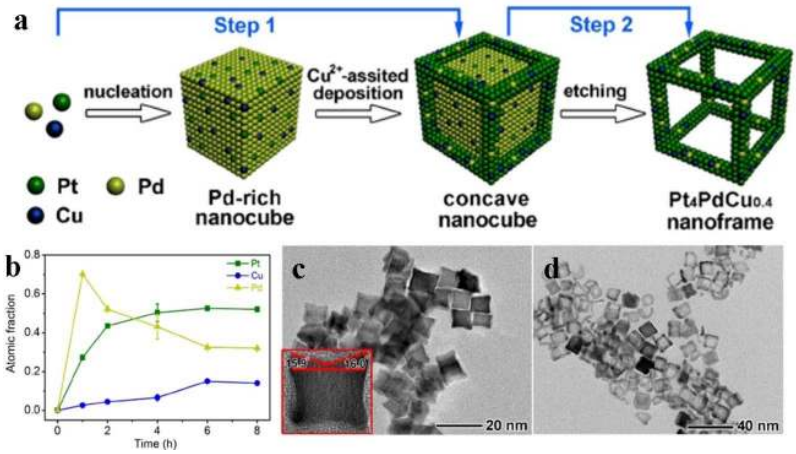

Fig. 4 (a) Schematic illustrating the formation process of PtPdCu concave nanocubes and NFs; (b) atomic ratio of the intermediate products in the formation stages of concave nanocubes; TEM images of (c) PtPdCu concave nanocubes and (d) PtPdCu NFs.

Adapted from Ref. 37, copyright 2017 Elsevier ScienceDirect.

economical with the uniform and regular Pt-based NFs crystals; however, it is limited to a short range of applications. The chemical etching can be applied in solid polyhedrons with richer metal components as compared to oxidative etching. In acid etching, Pt-based NFs can be achieved quickly by selecting different types and concentrations of acid liquids to corrode inner solid metal polyhedrons, while in organic etching different types and concentrations of organic solvents are selected to slowly etch the internal metal. The experimental period of acid etching is short, but the obtained crystal structure is easily damaged [36]. On the contrary, the organic etching period is more extended, but the synthesized crystal is relatively complete and robust. Additionally, galvanic replacement and carbon monoxide etching are rarely reported in the synthesis of Pt-based NFs, but they still have great development space and more possibilities. Although galvanic replacement and carbon monoxide etching are more complicated in experimental operations, they can effectively etch more stable metals and obtain richer Pt-based multi-component NFs, which cannot be achieved by oxidative etching and chemical etching.

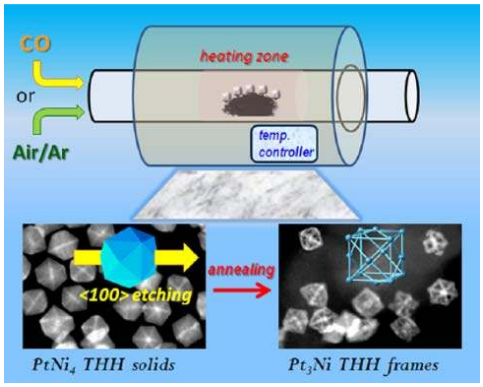

Fig. 5 Schematic illustrating the formation process of tetrahexahedral PtNi NFs, insets are TEM images for solid PtNi tetrahexahedron and PtNi tetrahexahedral NFs.

Adapted from Ref. 64, Copyright 2017 American Chemical Society.

4 Application of Pt-based NFs in DAFCs

DAFCs are promising clean energy sources where liquid alcohol is used as fuel which mainly composed of oxidation reaction of alcoholic fuels at anode and oxygen reduction at cathode. However, the alcohol oxidation poisoning (CO intermediates) and the limited oxidation efficiency (incomplete CO_2 and H_2O oxidation products), as well as the slow oxygen reduction kinetics and short cycle life hamper the further development of DAFCs. Pt-based NFs have been widely used in DAFCs electrocatalysis for ORR, MOR and EOR (Scheme 3) [76–78]. Table 2 presents a detailed overview of Pt-based NFs in DAFCs half-cell testing. The activity, durability and anti-poisoning ability of the Pt-based NFs can be improved in MOR, EOR and ORR due to the higher utilization of active sites, more open space structure, larger accessible surface, and multicomponent strain and synergistic effects [79–82].

4.1 Oxygen reduction reaction

A lot of efforts have been devoted to improve the slow kinetics of cathode ORR for the enhanced conversion efficiency and performance of the full cell with more economical accessibility. In this regard, numerous Pt-based NFs have been employed for

Scheme 3 Schematic illustration of Pt-based NFs in application of ORR, MOR and EOR for DAFCs.

Table 2 The reported catalytic applications of Pt-based NFs with various shapes and compositions.

Electrocatalytic reaction	Shape and composition of Pt-based NFs		
Oxygen reduction	Rhombic dodecahedral PtCu [32–34]	Rhombic dodecahedral PtCuNi [36]	Cubic PtPdCu [37]
	Octopod cubic PtCu [38]	Rhombic dodecahedral PtNi [44–47,83]	Cubic Pt [25,84]
	Five-Fold-Twinned PtCu [39]	Rhombic dodecahedral PtCo [55,85]	Tetrahexahedral PtNi [64]
	Vertex-Reinforced PtCuCo [24]	Spiny rhombic dodecahedral PtCu [49]	Skeletal octahedral PtNi [53]
	Octahedral PtCu [42]	Five-Fold-Twinned PtCuMn [43]	Dendrite-Embedded PtNi [62]
Methanol oxidation	Rhombic dodecahedral PtCuRh [41]	Rhombic dodecahedral PtCu [34,35]	Cubic PtCu [86]
	Concave cubic PtCu [40]	Five-Fold-Twinned PtCu [39]	Tetrahexahedral PtNi [23,64]
	Vertex-Reinforced PtCuCo [24]	Octahedral PtNi [26]	Truncated octahedronal PtNiAu [48]
	Rhombic dodecahedral PtRuNi [52]	Rhombic dodecahedral PtCo [55]	Octahedral PtCu [42]
	Core-Shell AgAuPt [57]	truncated octahedral PtAu [58]	AuPt bipyramid [59]
	Ultra-Small PtPdRhAg [60]		
Ethanol oxidation	Rhombic dodecahedral PtCuRh [41]	Vertex-Reinforced PtCuRh [50]	Porous Pt-Bi$(OH)_3$ [61]
	Rhombic dodecahedral PtRhNi [54]		

ORR in energy conversion technology [87–90]. The rhombic dodecahedral PtNi NFs reported by Yang's group advances the application of Pt-based NFs in ORR to an unprecedented level [44,46]. *In situ* structural evolution analysis of the PtNi NFs indicates that Pt species will gradually migrate to the edges and corners under crystal stress and other species' squeeze during the crystal growth process (Fig. 6a) [91–94]. At the etching stage, the internal metal is removed, leaving behind the hollow and excavated PtNi NFs structure with Pt-rich corners and edges (Fig. 6b). A precise EDS mapping further displays PtNi alloy edge, suggesting a slight loss of Pt in etching, and this effect is far less than the contribution of NFs to catalysis (Fig. 6c). PtNi NFs with Pt skin exhibited outstanding mass activity due to high active site utilization, open space structure and large accessible surface, which is ~9 times than that of Pt/C in the ORR evaluation (Fig. 6d) [95–97]. Moreover, PtNi alloy possesses lower Pt consumption and enhanced intrinsic stability due to lattice stress and synergistic effect. PtNi NFs have negligible structural and activity degradation during 10,000 cycles of accelerated durability test (ADT), further indicating the highly robust PtNi NFs possess superior ORR catalytic activity through weakening adsorption of Pt-O intermediates (Fig. 6e). Additionally, *in situ* X-ray absorption spectroscopy (XAS) detection analyzes the dynamic changes in the coordination and composition of PtNi NFs during ORR, indicating Pt-rich skin can strengthen the catalytic activity, weaken the adsorption energy between surface and adsorbates and relieve the Ni dissolution (Fig. 6f). Hence, PtNi NFs have promising potential towards improved activity and stability for the development and application of ORR [47,98]. Due to the mismatch of the crystal structure of Pt and Co, the preparation of PtCo alloys and heterostructures have been challenging (Fig. 6g). Recently, solid rhombohedral dodecahedrons were synthesized under anhydrous and oxygen-free conditions (Fig. 6h), and PtCo rhombic dodecahedron NFs were obtained under strong corrosion of nitric acid (Fig. 6i). Compared with commercial Pt/C, the half-wave potential of PtCo NFs have a positive shift of 26 mV and a negligible degradation during ADT (Fig. 6j). Moreover, the corresponding mass activity at 0.95 V of PtCo NFs is 4 times that of Pt/C, which exceeds the catalytic activity of previous PtNi NFs (Fig. 6k). The development of PtCo NFs provides a capable strategy for the Pt-based NFs with mismatched crystal structure.

Furthermore, vertex-reinforced PtCu cubic NFs are prepared through accelerated deposition on the corners (Fig. 6l). Numerous high-index facets possess lower coordination numbers and higher free energy compared to standard Pt, which can promote the molecular absorption and electron transfer in electrocatalysis (Fig. 6m). The vertex-reinforced PtCu NFs exhibit more superior half-wave potential with an outstanding mass activity of 20 times higher than Pt/C (Fig. 6n, o). In a word, the Pt-based NFs play a vital role in ORR due to efficient utilization of active sites, large accessible surface and open space structure, which facilitate efficient electron transfer, promote mass transport, weaken surface adsorption energies and improve the coordination environment.

4.2 Methanol oxidation reaction

In addition to ORR, the oxidation of small alcohol molecules is essential in DAFCs. Methanol is a simple alcoholic molecule has a fast oxidation pathway with 100% conversion efficiency. The representative PtNi octahedral NFs and porous octahedra for MOR are prepared by slow chemical etching (Fig. 7a, b). Compared with Pt/C catalyst, PtNi octahedral NFs exhibit higher intensity in peak current density and mass activity, indicating the highly open space structure and larger accessible surface facilitates the efficient electron transfer and mass transport (Fig. 7c, d). Meanwhile, truncated octahedron PtNi NFs are obtained with Au decoration to form PtNi-Au ternary NFs (Fig. 7e). Compared with solid PtNi truncated octahedron, truncated octahedron PtNi NFs show strengthening peak current density because of higher Pt atomic utilization and larger accessible surface (Fig. 7f). Furthermore, CO stripping experiments show that Au modified PtNi NFs have the earliest oxidation potential compared to PtNi NFs and solid PtNi, further demonstrating the outstanding resistance to CO poisoning (Fig. 7g). Au-PtNi NFs

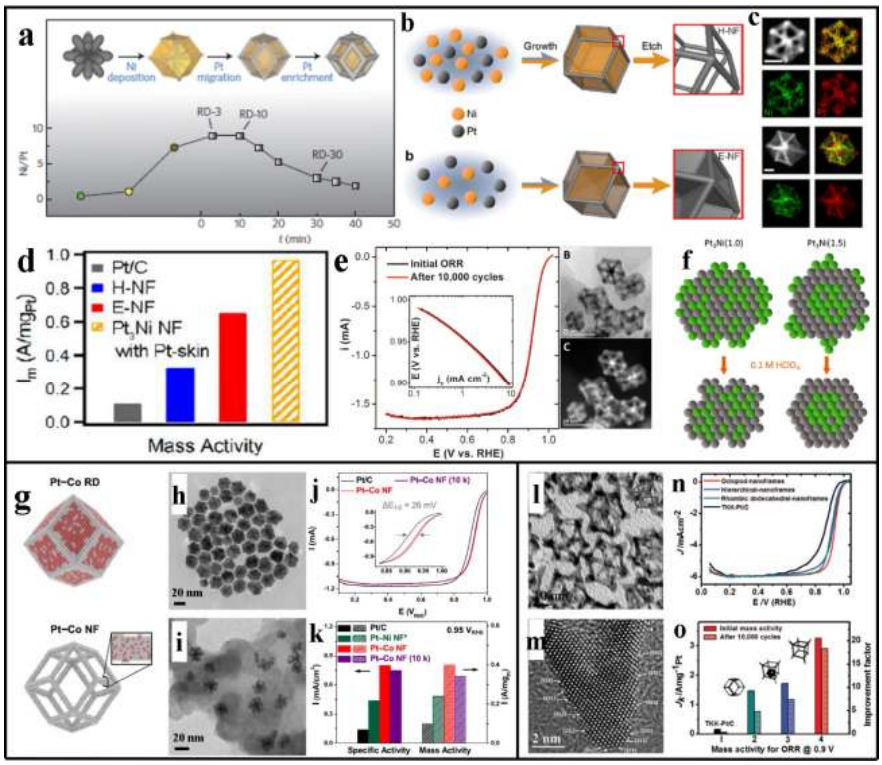

Fig. 6 (a) Summary of the complete growth process of a PtNi heterogeneous rhombic dodecahedron, and corresponding composition of Pt and Ni in the products; (b) structural evolution models, (c) EDS mapping and (d) mass activity of hollow and excavated PtNi NFs; (e) ORR polarization curves, Tafel plots and TEM images of PtNi NFs before and after ADT test; (f) *in situ* XAS detection model of PtNi NFs in the ORR process; (g) models of solid PtCo rhombic dodecahedrons and PtCo alloy NFs; TEM images of (h) solid PtCo rhombic dodecahedrons and (i) carbon-supported PtNi NFs. (j) ORR polarization curves and Tafel plots of PtCo NFs before and after ADT test; (k) mass activity and specific activity of Pt/C, PtCo NFs and PtNi NFs; (l) TEM image of Octopod PtCu NFs, (m) HRTEM image and matching high-index facets of the tip area; (n) ORR curves, (o) mass activity of Pt/C and PtCu NFs.

Panel a adapted from Ref. 91, copyright 2016 Nature group. Panels b–d adapted from Ref. 47, copyright 2017 American Chemical Society. Panel e adapted from Ref. 45, copyright 2014 American Association for the Advancement of Science. Panel f adapted from Ref. 44, copyright 2015 American Chemical Society. Panels g–k adapted from Ref. 55, copyright 2020 American Chemical Society. Panels l–o adapted from Ref. 38, copyright 2017 Wiley-VCH.

display a negligible degradation in extended cycling tests and a significant improvement relative to PtNi NFs, which is attributed to weakened surface adsorption, redesigned electronic structure and strengthening intrinsic stability (Fig. 7h). Moreover, PtCu concave and octopod cubic NFs are synthesized by the one-pot solvothermal method and oxidative etching [99–101]. Bromide ions are selectively adsorbed on the {110} surface of the cubic crystal which forms an oxidative etching pair with O molecules to remove internal Cu and maintain the external PtCu alloy to obtain complete PtCu NFs (Fig. 7i, j) [102]. The highly open PtCu octopod cubic NFs and some high-energy surfaces in the tip areas can be observed, with uniform edges and corners conducive to facilitate electron transfer, tip absorption and active site exposure. The peak current density of PtCu NFs with smaller onset potential is ~7 times than that of Pt/C, indicating an outstanding MOR activity (Fig. 7k). Also, PtCu NFs show superior catalytic activity in formic acid oxidation relative to Pt/C (Fig. 7l). Based on the results above, most of the synthesized NFs materials possess robust MOR catalytic activity, implying the realization of low-cost, efficient and stable electrocatalytic materials.

4.3 Ethanol oxidation reaction

As a liquid fuel, ethanol has the advantages of wide sources, easy transportation and storage, high energy density and eco-friendliness. However, the ethanol oxidation endures a stable C—C bond cleavage; hence the energy cannot be released quickly. Therefore, the development and application of ethanol oxidation have received much attention. Pt-based NFs are also widely applied in EOR and exhibit significant catalytic performance (Table 2). According to the synthesis recipe of PtCu NFs, rhombohedral PtCuRh NFs can be obtained by combining solvothermal, chemical corrosion and regulating the Rh addition (Fig. 8a). By increasing the temperature of the reaction system, the thermodynamics of the reaction and the rate of atom growth and deposition are accelerated, thereby obtaining multi-footed PtCuRh NFs with apex extension (Fig. 8b), where the apex exhibits a higher current intensity due to the tip effect, enlarged specific surface and more coordination options (Fig. 8c).

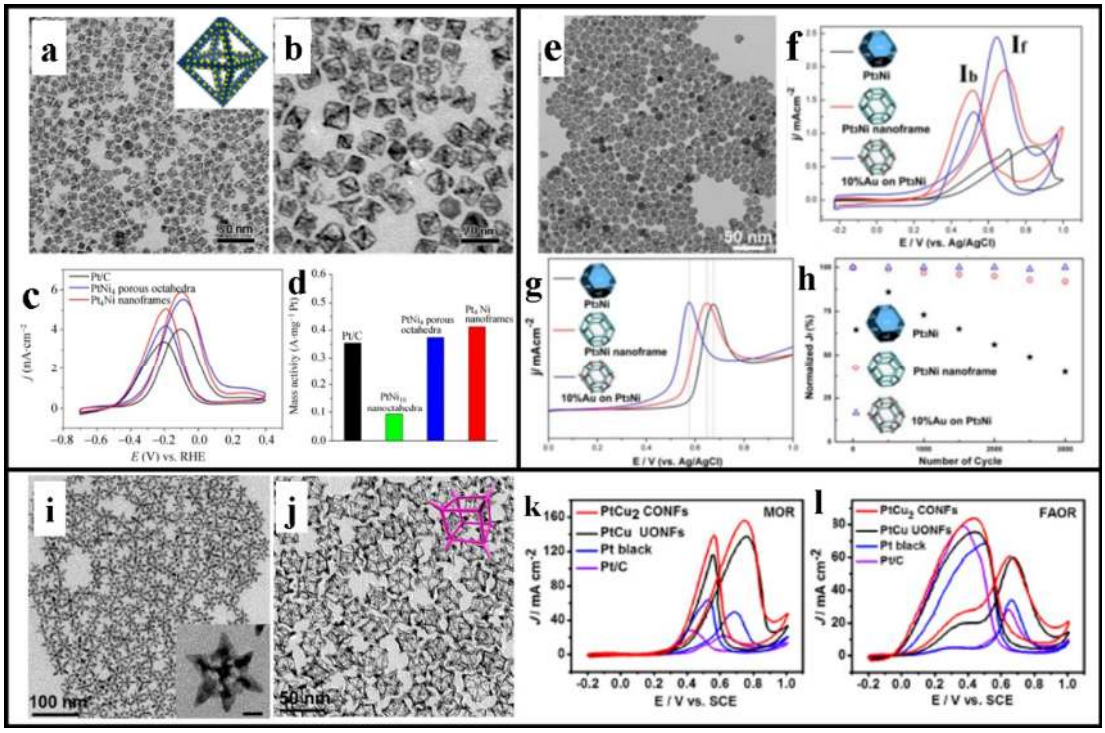

Fig. 7 (a) Low-, (b) high-magnification TEM images of PtNi octahedrons; (c) MOR curves, (d) mass activity of Pt/C, PtNi porous octahedrons and PtNi NFs; (e) TEM image of truncated octahedral PtNiAu NFs, (f) MOR curves, (g) CO-stripping and (h) ADT tests of PtNi truncated octahedrons, PtNi NFs, PtNiAu NFs; TEM images of (i) PtCu concave cubic NFs and (j) PtCu octopod cubic NFs; (k) MOR curves and (l) FAOR curves of Pt/C, Pt black, PtCu concave cubic and octopod NFs.

Panels a–d adapted from Ref. 26, copyright 2014 Springer-Verlag. Panels e–h adapted from Ref. 48, copyright 2014 American Chemical Society, Panels i–l adapted from Ref. 40, copyright 2016 American Chemical Society.

Relative to PtCuRh NFs, multi-footed PtCuRh NFs have significant enhancement in activity and attenuation of multi-footed PtCuRh NFs is also smaller in the long-term durability test (Fig. 8d). Besides, vertex-reinforced PtCuRh solid polyhedrons are prepared through crystal growth and corner deposition, followed by the oxidative and acid etching to obtain hollow PtCuRh NFs with the more prominent bright edges (Fig. 8e) [50]. High atomic utilization, open space structure and large specific surface areas along with high-index facets of vertex-reinforced structure facilitate efficient mass transport and electron transfer in electrocatalysis for the improved EOR (Fig. 8f, g) [103–105]. Compared with PtCu nanocrystals and PtCuRh nanoparticles, vertex-reinforced PtCuRh NFs achieve an enhanced current density due to more active sites and coordination options. Also, the introduction of Rh promotes the oxidation of ethanol, which provides a direction for breaking C—C bonds and the full oxidation of ethanol [54,106]. More importantly, the anti-poisoning ability is an essential parameter to assess the sustainable performance of catalysts in alcohol oxidation, especially the strong adsorption of CO on the catalytic surface during the reaction, where the oxidation peak potential and onset potential of PtCuRh materials are more negative compared to commercial Pt/C and PtCu material (Fig. 8h). Compared with PtCu and Pt/C materials, PtCuRh NFs exhibit more outstanding life time, reaction intensity and poison tolerance, implying the introduction of Rh species can strengthen the reaction efficiency and stability of Pt catalysts. Additionally, PtNi tetrahexahedron and rhombic dodecahedron achieve a conversion from solid nanocrystals to hollow NFs by long-term acid etching (Fig. 8i). Noticeably, controllable PtNi NFs as multifunctional catalysts are broadly invested in ORR, MOR and EOR. Compared with Pt/C catalyst, PtNi NFs possess more positive onset and half-wave potential for ORR, implying a better catalytic activity (Fig. 8j). Also, PtNi NFs exhibit higher oxidation intensity than Pt/C in MOR and EOR, demonstrating a significant enhancement of its catalytic oxidation efficiency (Fig. 8k, l). Pt-based NFs show not only outstanding catalytic performance in ORR but also strong catalytic efficiency in the oxidation of small alcohol molecules.

Pt materials as one of the most representative catalysts have been widely used in many electrocatalytic reactions, nevertheless high cost and limited resources severely hinder the development and application of Pt-based catalysts. The development of Pt-based NFs materials has achieved decreased Pt consumption, the greatly improved Pt utilization and the enhanced catalytic performance. Through the discussion of typical Pt-based NFs, we have concluded that Pt-based NFs can be widely used in ORR, MOR and EOR for DAFCs, which is a promising frontier technology in future sustainable energy technologies. Consequently, Pt-based NFs will usher in a longer-

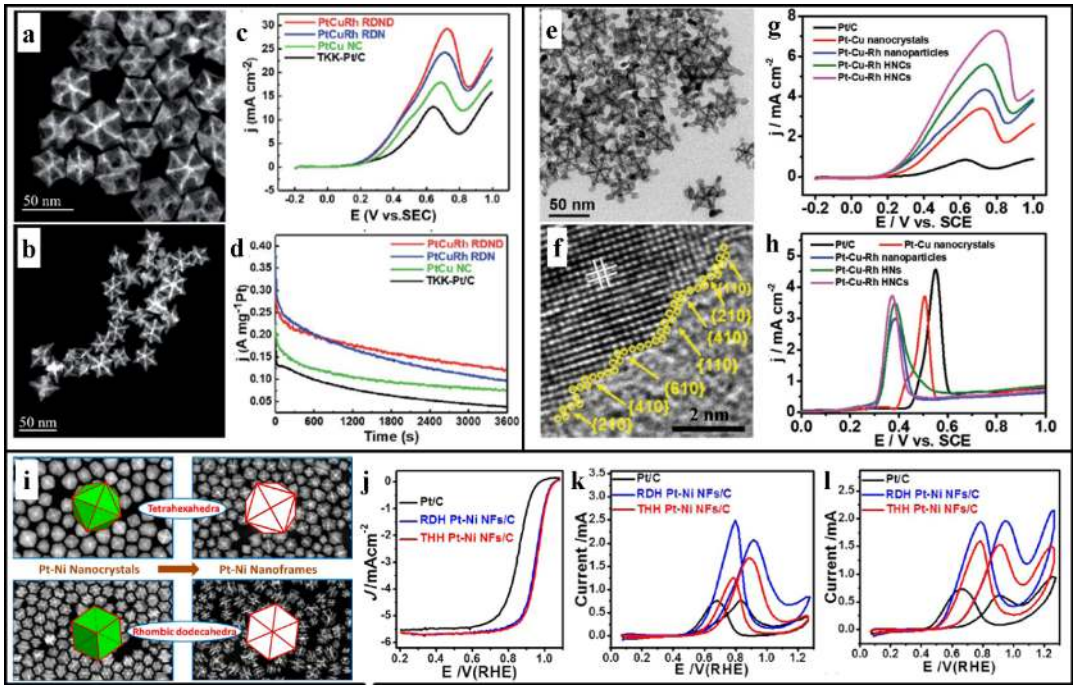

Fig. 8 HAADF-STEM images of (a) PtCuRh NFs and (b) multi-footed PtCuRh NFs; (c) EOR curves, (d) the durability tests of PtCuRh NFs, PtCu NFs and Pt/C; (e) TEM image, (f) HRTEM image of vertex-reinforced PtCuRh NFs; (g) EOR curves, (h) anti-poisoning ability measurements of Pt/C, PtCu, PtCuRh nanoparticles and vertex-reinforced PtCuRh NFs; (i) structural evolution from PtNi nanocrystals to PtNi NFs, (j) ORR curves, (k) MOR curves and (l) EOR curves of Pt/C and PtNi NFs.

Panels a–d adapted from Ref. 41, copyright 2019 Royal Society of Chemistry, Panels e–h adapted from Ref. 50, copyright 2018 Wiley-VCH.

Panels i–l adapted from Ref. 23, copyright 2016 American Chemical Society.

term development and is expected to serve as a multi-purpose c atalyst to meet DAFCs applications.

5 Perspective and outlook

Pt-based NFs can be mainly prepared by four prominent etching strategies (oxidative etching, electrical replacement, chemical etching, and carbon monoxide etching) based on binary and multicomponent heterogeneous solid polyhedral nanocrystals. Notably, Pt-based NFs are regarded as one of the most efficient electrocatalysts in numerous energy conversion fields (ORR, MOR, EOR) due to the highly open space structure, large specific surface areas, efficient Pt utilization and full accessible active sites. Although the cost reduction and performance improvement of Pt-based NFs have achieved phased results in recent years, there is still a lot of research and development space for the industrial preparation method, commercial application and continuous optimization of the cost and performance of catalytic materials. In addition to PtCu, the PtNi-based NFs can be efficiently prepared; however, the effective preparation and accurate etching of more binary and multivariate Pt-based NFs is still a considerable challenge. Especially, when PtCo catalysts have begun to be commercialized in fuel cell vehicles, efficient scale-up synthesis methods for the preparation of PtCo NFs are still lacking. Likewise, it is necessary to reduce the particle size and thickness of NFs, which can add extra rise to the specific surface area of the materials and the utilization rate of Pt atoms, thereby reducing the material cost of the catalyst and improving the catalytic activity. Furthermore, it might be feasible to introduce carbon monoxide etching methods into the etching techniques. The current work shows much room for the development of NFs architecture, especially the etching mechanism of carbon monoxide and the application scope of more alloying composition. More importantly, the carbon monoxide etching can avoid all surfactants and organic solvents, which leads to a cleaner surface of the nanocrystals for the full use of active sites.

Facing the vast new energy market, researchers should commit to develop novel synthesis techniques and further obtain better catalytic materials by optimizing the structure of Pt-based NFs catalysts to advance the Pt utilization, introducing other non-precious metals to reduce the Pt consumption, and further reducing the size of Pt-based NFs to strengthen the catalytic activity and stability of the catalyst. More meaningfully, the development of DAFCs and Pt-based NFs involves the life time, catalytic activity and anti-poisoning ability in acidic conditions, which can be further strengthened through small-sized fabrication, Pt-rich skin construction, high-energy area design and Pt-C integrated investigation (Scheme 4). Moreover, the scientific issues in anodic alcohol oxidation and cathodic oxygen reduction need to be clarified, such as product detection, reaction mechanism and structure-activity relationship. Also, *in-situ* characterization methods, simulation calculations and artificial

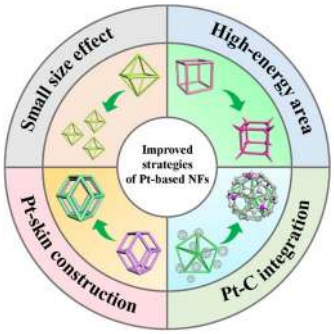

Scheme 4 Schematic illustration of improved strategies for Pt-based NFs.

intelligence can be considered further to realize real-time monitoring of material synthesis and reaction processes, simulation of the microscopic molecular environment and surface adsorption, big data screening and machine learning, which is conducive to clearly understand the dynamic process and digital analysis of reaction pathway. Meanwhile, the scale-up synthesis strategy of catalyst, membrane electrode assembly, development of start-stop system and design of the circulation system are essential for the commercial application and industrial manufacturing of DAFCs. We believe the continuous optimization and improvement in Pt-based NFs will bring a promising future for DAFCs in energy conversion technologies.

References

(1) Choi, S. I.; Shao, M.; Lu, N.; Ruditskiy, A.; Peng, H. C.; Park, J.; Guerrero, S.; Wang, J.; Kim, M. J.; Xia, Y. *ACS Nano* **2014,** *8*, 10363. doi: 10.1021/nn5036894

(2) Huang, L.; Wei, M.; Hu, N.; Tsiakaras, P.; Shen, P. K. *Appl. Catal. B. Environ.* **2019,** *258*, 117974. doi: 10.1016/j.apcatb.2019.117974

(3) Li, M. G.; Xia, Z. H.; Huang, Y. R.; Tao, L.; Chao, Y. G.; Yin, K.; Yang, W. X.; Yang, W. W.; Yu, Y. S.; Guo, S. J. *Acta Phys. -Chim. Sin.* **2020,** *36*, 1912049. [李蒙刚, 夏仲泓, 黄雅荣, 陶璐, 晁玉广, 尹坤, 杨文秀, 杨微微, 于永生, 郭少军. 物理化学学报 **2020,** *36*, 1912049.] doi: 10.3866/PKU.WHXB201912049

(4) Lv, L.; Zhang, L. Y.; He, X. B.; Yuan, H.; Ouyang, S. X.; Zhang, T. R. *Acta Phys. -Chim. Sin.* **2021,** *37*, 2007079. [吕琳, 张立阳, 何雪冰, 原弘, 欧阳述昕, 张铁锐. 物理化学学报, **2021,** *37*, 2007079.] doi: 10.3866/PKU.WHXB202007079

(5) Zhang, Y. J.; Zhu, Y. Z.; Li, J. F. *Acta Phys. -Chim. Sin.* **2021,** *37*, 2004052. [张月皎, 朱越洲, 李剑锋. 物理化学学报, **2021,** *37*, 2004052.] doi: 10.3866/PKU.WHXB202004052

(6) Kongkanand, A.; Mathias, M. F. *J. Phys. Chem. Lett.* **2016,** *7*, 1127. doi: 10.1021/acs.jpclett.6b00216

(7) Ma, S. Y.; Li, H. H.; Hu, B. C.; Cheng, X.; Fu, Q. Q.; Yu, S. H. *J. Am. Chem. Soc.* **2017,** *139*, 5890. doi: 10.1021/jacs.7b01482

(8) Li, K. X.; Zhang, T. L.; Li, H. Z.; Li, M. Z.; Song, Y. L. *Acta Phys. -Chim. Sin.* **2020,** *36*, 1911057. [李凯旋, 张泰隆, 李会增, 李明珠, 宋延林. 物理化学学报, **2020,** *36*, 1911057.] doi: 10.3866/PKU.WHXB201911057

(9) Kang, Y.; Snyder, J.; Chi, M.; Li, D.; More, K. L.; Markovic, N. M.; Stamenkovic,V. R. *Nano Lett.* **2014,** *14*, 6361. doi: 10.1021/nl5028205

(10) Tang, Z. Y. *Acta Phys. -Chim. Sin.* **2020,** *36*, 2004050. [唐智勇. 物理化学学报, **2020,** *36*, 2004050.] doi: 10.3866/PKU.WHXB202004050

(11) You, H.; Yang, S.; Ding, B.; Yang, H. *Chem. Soc. Rev.* **2013,** *42*, 2880. doi: 10.1039/C2CS35319A

(12) Shi, Y.; Lyu, Z.; Zhao, M.; Chen, R.; Nguyen, Q. N.; Xia, Y. *Chem. Rev.* **2020,** doi: 10.1021/acs.chemrev.0c00454

(13) Kwon, T.; Jun, M.; Lee, K. *Adv. Mater.* **2020,** *32*, 2001345. doi: 10.1002/adma.202001345

(14) Park, J.; Kanti Kabiraz, M.; Kwon, H.; Park, S.; Baik, H.; Choi, S. I.; Lee, K. *ACS Nano* **2017,** *11*, 10844. doi: 10.1021/acsnano.7b04097

(15) Yang, T. Y.; Cui, C.; Rong, H. P.; Zhang, J. T.; Wang, D. S. *Acta Phys. -Chim. Sin.* **2020,** *36*, 2003047. [杨天怡, 崔铖, 戎宏盼, 张加涛, 王定胜. 物理化学学报, **2020,** *36*, 2003047.] doi: 10.3866/PKU.WHXB202003047

(16) Zhang, L.; Roling, L. T.; Wang, X.; Vara, M.; Chi, M.; Liu, J.; Choi, S. I.; Park, J.; Herron, J. A.; Xie, Z.; *et al*. *Science* **2015,** *349*, 412. doi: 10.1126/science.aab0801

(17) Nosheen, F.; Zhang, Z. C.; Zhuang, J.; Wang, X. *Nanoscale* **2013,** *5*, 3660. doi: 10.1039/C3NR00833A

(18) Carpenter, M. K.; Moylan, T. E.; Kukreja, R. S.; Atwan, M. H.; Tessema, M. M. *J. Am. Chem. Soc.* **2012,** *134*, 8535. doi: 10.1021/ja300756y

(19) Mourdikoudis, S.; Liz-Marzán, L. M. *Chem. Mater.* **2013,** *25*, 1465. doi: 10.1021/cm4000476

(20) Liu, H. L.; Nosheen, F.; Wang, X. *Chem. Soc. Rev.* **2015,** *44*, 3056. doi: 10.1039/C4CS00478G

(21) Kong, F.; Ren, Z.; Norouzi Banis, M.; Du, L.; Zhou, X.; Chen, G.; Zhang, L.; Li, J.; Wang, S.; Li, M.; *et al*. *ACS Catal.* **2020,** *10*, 4205. doi: 10.1021/acscatal.9b05133

(22) Liu, M. M.; Yang, M. M.; Shu, X. X.; Zhang, J. T. *Acta Phys. -Chim. Sin.* **2021,** *37*, 2007072. [刘苗苗, 杨茅茂, 舒欣欣, 张进涛. 物理化学学报, **2021,** *37*, 2007072.] doi: 10.3866/PKU.WHXB202007072

(23) Ding, J.; Bu, L.; Guo, S.; Zhao, Z.; Zhu, E.; Huang, Y.; Huang, X. *Nano Lett.* **2016,** *16*, 2762. doi: 10.1021/acs.nanolett.6b00471

(24) Kwon, T.; Jun, M.; Kim, H. Y.; Oh, A.; Park, J.; Baik, H.; Joo, S. H.; Lee, K. *Adv. Funct. Mater.* **2018,** *28*, 1706440. doi: 10.1002/adfm.201706440

(25) Park, J.; Wang, H.; Vara, M.; Xia, Y. *ChemSusChem* **2016,** *9*, 2855. doi: 10.1002/cssc.201600984

(26) Wang, Y.; Chen, Y.; Nan, C.; Li, L.; Wang, D.; Peng, Q.; Li, Y. *Nano Res.* **2014,** *8*, 140. doi: 10.1007/s12274-014-0603-z

(27) Beermann, V.; Holtz, M. E.; Padgett, E.; de Araujo, J. F.; Muller, D. A.; Strasser, P. *Energy Environ. Sci.* **2019,** *12*, 2476. doi: 10.1039/C9EE01185D

(28) Cui, C.; Gan, L.; Heggen, M.; Rudi, S.; Strasser, P. *Nat. Mater.* **2013,** *12*, 765. doi: 10.1038/nmat3668

(29) Zhu, C.; Du, D.; Eychmuller, A.; Lin, Y. *Chem. Rev.* **2015,** *115*, 8896. doi: 10.1021/acs.chemrev.5b00255

(30) Bu, L.; Guo, S.; Zhang, X.; Shen, X.; Su, D.; Lu, G.; Zhu, X.; Yao, J.; Guo, J.; Huang, X. *Nat. Commun.* **2016,** *7*, 11850. doi: 10.1038/ncomms11850

(31) Godinez-Salomon, F.; Mendoza-Cruz, R.; Arellano-Jimenez, M. J.; Jose-Yacaman, M.; Rhodes, C. P. *ACS Appl. Mater. Interfaces* **2017,** *9*, 18660. doi: 10.1021/acsami.7b00043

(32) Huang, X. Y.; You, L. X.; Zhang, X. F.; Feng, J. J.; Zhang, L.; Wang, A. J. *Electrochim. Acta* **2019,** *299*, 89. doi: 10.1016/j.electacta.2019.01.002

(33) Niu, H. J.; Chen, H. Y.; Wen, G. L.; Feng, J. J.; Zhang, Q. L.; Wang, A. J. *J. Colloid. Interface Sci.* **2019,** *539*, 525. doi: 10.1016/j.jcis.2018.12.066

(34) Sun, X.; Huang, B.; Cui, X.; E, B.; Feng, Y.; Huang, X. *ChemCatChem* **2018,** *10*, 931. doi: 10.1002/cctc.201701768

(35) Ding, J.; Zhu, X.; Bu, L.; Yao, J.; Guo, J.; Guo, S.; Huang, X. *Chem. Commun.* **2015,** *51*, 9722. doi: 10.1039/C5CC03190G

(36) Huang, L.; Jiang, Z.; Gong, W.; Wang, Z.; Shen, P. K. *J. Power Sources* **2018,** *406*, 42. doi: 10.1016/j.jpowsour.2018.10.041

(37) Ye, W.; Chen, S.; Ye, M.; Ren, C.; Ma, J.; Long, R.; Wang, C.; Yang, J.; Song, L.; Xiong, Y. *Nano Energy* **2017,** *39*, 532. doi: 10.1016/j.nanoen.2017.07.025

(38) Luo, S.; Tang, M.; Shen, P. K.; Ye, S. *Adv. Mater.* **2017,** *29*, 1601687. doi: 10.1002/adma.201601687

(39) Zhang, Z.; Luo, Z.; Chen, B.; Wei, C.; Zhao, J.; Chen, J.; Zhang, X.; Lai, Z.; Fan, Z.; Tan, C.; *et al*. *Adv. Mater.* **2016,** *28*, 8712. doi: 10.1002/adma.201603075

(40) Luo, S.; Shen, P. K. *ACS Nano* **2017,** *11*, 11946. doi: 10.1021/acsnano.6b04458

(41) Wang, Z.; Huang, L.; Tian, Z. Q.; Shen, P. K. *J. Mater. Chem. A* **2019,** *7*, 18619. doi: 10.1039/C9TA06119C

(42) Zhu, G.; Liu, J.; Li, S.; Zuo, Y.; Li, D.; Han, H. *ACS Appl. Energy Mater.* **2019,** *2*, 2862. doi: 10.1021/acsaem.9b00205

(43) Qin, Y.; Zhang, W.; Guo, K.; Liu, X.; Liu, J.; Liang, X.; Wang, X.; Gao, D.; Gan, L.; Zhu, Y.; *et al*. *Adv. Funct. Mater.* **2020,** *30*, 1910107. doi: 10.1002/adfm.201910107

(44) Becknell, N.; Kang, Y.; Chen, C.; Resasco, J.; Kornienko, N.; Guo, J.; Markovic, N. M.; Somorjai, G. A.; Stamenkovic, V. R.; Yang, P. *J. Am. Chem. Soc.* **2015,** *137*, 15817. doi: 10.1021/jacs.5b09639

(45) Chen, C.; Kang, Y.; Huo, Z.; Zhu, Z.; Huang, W.; Xin, H. L.; Snyder, J. D.; Li, D.; Herron, J. A.; Mavrikakis, M.; Chi, M.; *et al*. *Science* **2014,** *343*, 1339. doi: 10.1126/science.1249061

(46) Chen, S.; Niu, Z.; Xie, C.; Gao, M.; Lai, M.; Li, M.; Yang, P. *ACS Nano* **2018,** *12*, 8697. doi: 10.1021/acsnano.8b04674

(47) Becknell, N.; Son, Y.; Kim, D.; Li, D.; Yu, Y.; Niu, Z.; Lei, T.; Sneed, B. T.; More, K. L.; Markovic, N. M.; *et al*. *J. Am. Chem. Soc.* **2017,** *139*, 11678. doi: 10.1021/jacs.7b05584

(48) Wu, Y.; Wang, D.; Zhou, G.; Yu, R.; Chen, C.; Li, Y. *J. Am. Chem. Soc.* **2014,** *136*, 11594. doi: 10.1021/ja5058532

(49) Lyu, L. M.; Kao, Y. C.; Cullen, D. A.; Sneed, B. T.; Chuang, Y. C.; Kuo, C. H. *Chem. Mater.* **2017,** *29*, 5681. doi: 10.1021/acs.chemmater.7b01550

(50) Wang, K.; Du, H.; Sriphathoorat, R.; Shen, P. K. *Adv. Mater.* **2018,** *30*, e1804074. doi: 10.1002/adma.201804074

(51) Ren, F.; Wang, Z.; Luo, L.; Lu, H.; Zhou, G.; Huang, W.; Hong, X.; Wu, Y.; Li, Y. *Chem. Eur. J.* **2015,** *21*, 13181. doi: 10.1002/chem.201501923

(52) Shang, C.; Guo, Y.; Wang, E. *J. Mater. Chem. A* **2019,** *7*, 2547. doi: 10.1039/C9TA00191C

(53) Oh, A.; Baik, H.; Choi, D. S.; Cheon, J. Y.; Kim, B.; Kim, H.; Kwon, S. J.; Joo, S. H.; Jung, Y.; Lee, K. *ACS Nano* **2015,** *9*, 2856. doi: 10.1021/nn5068539

(54) Gruzel, G.; Piekarz, P.; Pawlyta, M.; Donten, M.; Parlinska-Wojtan, M. *ACS Appl. Mater. Interfaces* **2019,** *11*, 22352. doi: 10.1021/acsami.9b04690

(55) Chen, S.; Li, M.; Gao, M.; Jin, J.; van Spronsen, M. A.; Salmeron, M. B.; Yang, P. *Nano Lett.* **2020,** *20*, 1974. doi: 10.1021/acs.nanolett.9b05251

(56) Becknell, N.; Zheng, C.; Chen, C.; Yu, Y.; Yang, P. *Surf. Sci.* **2016,** *648*, 328. doi: 10.1016/j.susc.2015.09.024

(57) Yan, X.; Yu, S.; Tang, Y.; Sun, D.; Xu, L.; Xue, C. *Nanoscale* **2018,** *10*, 2231. doi: 10.1039/C7NR08899J

(58) Yoo, S.; Cho, S.; Kim, D.; Ih, S.; Lee, S.; Zhang, L.; Li, H.; Lee, J. Y.; Liu, L.; Park, S. *Nanoscale* **2019,** *11*, 2840. doi: 10.1039/C8NR08231F

(59) Fang, C.; Zhao, G.; Zhang, Z.; Ding, Q.; Yu, N.; Cui, Z.; Bi, T. *Chem. Eur. J.* **2019**, *25*, 7351. doi: 10.1002/chem.201900403

(60) Saleem, F.; Ni, B.; Yong, Y.; Gu, L.; Wang, X. *Small* **2016**, *12*, 5261. doi: 10.1002/smll.201601299

(61) Yuan, X.; Jiang, B.; Cao, M.; Zhang, C.; Liu, X.; Zhang, Q.; Lyu, F.; Gu, L.; Zhang, Q. *Nano Res.* **2020**, *13*, 265. doi: 10.1007/s12274-019-2609-z

(62) Kwon, H.; Kabiraz, M. K.; Park, J.; Oh, A.; Baik, H.; Choi, S. I.; Lee, K. *Nano Lett.* **2018**, *18*, 2930. doi: 10.1021/acs.nanolett.8b00270

(63) Tsuji, M.; Hamasaki, M.; Yajima, A.; Hattori, M.; Tsuji, T.;

Kawazumi, H. *Mater. Lett.* **2014**, *121*, 113. doi: 10.1016/j.matlet.2014.01.093

(64) Wang, C.; Zhang, L.; Yang, H.; Pan, J.; Liu, J.; Dotse, C.; Luan, Y.; Gao, R.; Lin, C.; Zhang, J.; *et al*. *Nano Lett.* **2017,** *17*, 2204. doi: 10.1021/acs.nanolett.6b04731

(65) Zheng, Y.; Zeng, J.; Ruditskiy, A.; Liu, M.; Xia, Y. *Chem. Mater.* **2013,** *26*, 22. doi: 10.1021/cm402023g

(66) Yu, X.; Li, L.; Su, Y.; Jia, W.; Dong, L.; Wang, D.; Zhao, J.; Li, Y. *Chem. Eur. J.* **2016,** *22*, 4960. doi: 10.1002/chem.201600079

(67) Liao, H. G.; Zherebetskyy, D.; Xin, H.; Czarnik, C.; Ercius, P.; Elmlund, H.; Pan, M.; Wang, L. W.; Zheng, H. *Science* **2014,** *345*, 916. doi: 10.1126/science.1253149

(68) Zhou, J.; Yang, Y.; Yang, Y.; Kim, D. S.; Yuan, A.; Tian, X.; Ophus, C.; Sun, F.; Schmid, A. K.; Nathanson, M.; *et al*. *Nature* **2019,** *570*, 500. doi: 10.1038/s41586-019-1317-x

(69) Wang, D.; Li, Y. *Adv. Mater.* **2011,** *23*, 1044. doi: 10.1002/adma.201003695

(70) Gan, L.; Cui, C.; Heggen, M.; Dionigi, F.; Rudi, S.; Strasser, P. *Science* **2014,** *346*, 1502. doi: 10.1126/science.1261212

(71) Chen, M.; Wu, B.; Yang, J.; Zheng, N. *Adv. Mater.* **2012,** *24*, 862. doi: 10.1002/adma.201104145

(72) Xu, X.; Zhang, X.; Sun, H.; Yang, Y.; Dai, X.; Gao, J.; Li, X.; Zhang, P.; Wang, H. H.; Yu, N. F.; Sun, S. G. *Angew. Chem. Int. Ed.* **2014,** *53*, 12522. doi: 10.1002/ange.201406497

(73) Jin, H.; Hong, Y.; Yoon, J.; Oh, A.; Chaudhari, N. K.; Baik, H.; Joo, S. H.; Lee, K. *Nano Energy* **2017,** *42*, 17. doi: 10.1016/j.nanoen.2017.10.033

(74) Sun, X.; Jiang, K.; Zhang, N.; Guo, S.; Huang, X. *ACS Nano* **2015,** *9*, 7634. doi: 10.1021/acsnano.5b02986

(75) Ahmadi, M.; Cui, C.; Mistry, H.; Strasser, P.; Cuenya, B. R. *ACS Nano* **2015,** *9*, 10686. doi: 10.1021/acsnano.5b01807

(76) Hong, J. W.; Kim, Y.; Wi, D. H.; Lee, S.; Lee, S. U.; Lee, Y. W.; Choi, S. I.; Han, S. W. *Angew. Chem. Int. Ed.* **2016,** *55*, 2753. doi: 10.1002/anie.201510460

(77) Saleem, F.; Zhang, Z.; Xu, B.; Xu, X.; He, P.; Wang, X. *J. Am. Chem. Soc.* **2013,** *135*, 18304. doi: 10.1021/ja4101968

(78) Li, Y.; Quan, F.; Chen, K.; Chen, L.; Chen, C. *Catal. Today* **2016,** *278*, 247. doi: 10.1016/j.cattod.2016.01.047

(79) Wang, X.; Vara, M.; Luo, M.; Huang, H.; Ruditskiy, A.; Park, J.; Bao, S.; Liu, J.; Howe, J.; Chi, M.; *et al*. *J. Am. Chem. Soc.* **2015,** *137*, 15036. doi: 10.1021/jacs.5b10059

(80) Zhu, J.; Xie, M.; Chen, Z.; Lyu, Z.; Chi, M.; Jin, W.; Xia, Y. *Adv. Energy Mater.* **2020,** *10*, 1904114. doi: 10.1002/aenm.201904114

(81) Luo, X.; Liu, C.; Wang, X.; Shao, Q.; Pi, Y.; Zhu, T.; Li, Y.; Huang, X. *Nano Lett.* **2020,** *20*, 1967. doi: 10.1021/acs.nanolett.9b05250

(82) Huang, L.; Zhang, X.; Han, Y.; Wang, Q.; Fang, Y.; Dong, S. *Chem. Mater.* **2017,** *29*, 4557. doi: 10.1021/acs.chemmater.7b01282

(83) Wang, Y.; Chen, S.; Wang, X.; Rosen, A.; Beatrez, W.; Sztaberek, L.; Tan, H.; Zhang, L.; Koenigsmann, C.; Zhao, J. *ACS Appl. Energy Mater.* **2020,** *3*, 768. doi: 10.1021/acsaem.9b01930

(84) Xia, B. Y.; Wu, H. B.; Wang, X.; Lou, X. W. *Angew. Chem. Int. Ed.* **2013,** *52*, 12337. doi: 10.1002/anie.201307518

(85) Zhu, X.; Huang, L.; Wei, M.; Tsiakaras, P.; Shen, P. K. *Appl. Catal. B. Environ.* **2021,** *281*, 119460. doi: 10.1016/j.apcatb.2020.119460

(86) Xia, B. Y.; Wu, H. B.; Wang, X.; Lou, X. W. *J. Am. Chem. Soc.* **2012,** *134*, 13934. doi: 10.1021/ja3051662

(87) Lin, R.; Cai, X.; Zeng, H.; Yu, Z. *Adv. Mater.* **2018,** *30*, e1705332. doi: 10.1002/adma.201705332

(88) Liu, M.; Zhao, Z.; Duan, X.; Huang, Y. *Adv. Mater.* **2019,** *31*, 1802234. doi: 10.1002/adma.201802234

(89) Liu, L.; Samjeské, G.; Takao, S.; Nagasawa, K.; Iwasawa, Y. *J. Power Sources* **2014,** *253*, 1. doi: 10.1016/j.jpowsour.2013.12.028

(90) Wang, D.; Xin, H. L.; Hovden, R.; Wang, H.; Yu, Y.; Muller, D. A.; DiSalvo, F. J.; Abruna, H. D. *Nat. Mater.* **2013,** *12*, 81. doi: 10.1038/nmat3458

(91) Niu, Z.; Becknell, N.; Yu, Y.; Kim, D.; Chen, C.; Kornienko, N.; Somorjai, G. A.; Yang, P. *Nat. Mater.* **2016,** *15*, 1188. doi: 10.1038/nmat4724

(92) Huang, X.; Zhao, Z.; Cao, L.; Chen, Y.; Zhu, E.; Lin, Z.; Li, M.; Yan, A.; Zettl, A.; Wang, Y. M.; *et al*. *Science* **2015,** *348*, 1230. doi: 10.1126/science.aaa8765

(93) Lim, B.; Jiang, M.; Camargo, P. H. C.; Cho, E. C.; Tao, J.; Lu, X.; Zhu, Y.; Xia,Y. *Science* **2009,** *324*, 1302. doi: 10.1126/science.1170377

(94) Strasser, P.; Koh, S.; Anniyev, T.; Greeley, J.; More, K.; Yu, C.; Liu, Z.; Kaya, S.; Nordlund, D.; Ogasawara, H.; *et al*. *Nat. Chem.* **2010,** *2*, 454. doi: 10.1038/nchem.623

(95) Stamenkovic, V. R.; Fowler, B.; Mun, B. S.; Wang, G.; Ross, P. N.; Lucas, C. A.; Markovic, N. M. *Science* **2007,** *315*, 493. doi: 10.1126/science.1135941

(96) Bu, L.; Zhang, N.; Guo, S.; Zhang, X.; Li, J.; Yao, J.; Wu, T.; Lu, G.; Ma, J. Y.; Su, D.; Huang, X. *Science* **2016,** *354*, 1410. doi: 10.1126/science.aah6133

(97) Tian, X.; Zhao, X.; Su, Y. Q.; Wang, L.; Wang, H.; Dang, D.; Chi, B.; Liu, H.; Hensen, E. J. M.; Lou, X. W. D.; Xia, B. Y. *Science* **2019,** *366*, 850. doi: 10.1126/science.aaw7493

(98) Pizzutilo, E.; Knossalla, J.; Geiger, S.; Grote, J. P.; Polymeros, G.; Baldizzone, C.; Mezzavilla, S.; Ledendecker, M.; Mingers, A.; Cherevko, S.; *et al*. *Adv. Energy Mater.* **2017,** *7*, 1700835. doi: 10.1002/aenm.201700835

(99) Cao, Y.; Yang, Y.; Shan, Y.; Huang, Z. *ACS Appl. Mater. Interfaces* **2016,** *8*, 5998. doi: 10.1021/acsami.5b11364

(100) Sneed, B. T.; Young, A. P.; Jalalpoor, D.; Golden, M. C.; Mao, S.; Jiang, Y.; Wang, Y.; Tsung, C. K. *ACS Nano* **2014,** *8*, 7239. doi: 10.1021/nn502259g

(101) Gunji, T.; Tanabe, T.; Jeevagan, A. J.; Usui, S.; Tsuda, T.; Kaneko, S.; Saravanan, G.; Abe, H.; Matsumoto, F. *J. Power Sources* **2015,** *273*, 990. doi: 10.1016/j.jpowsour.2014.09.182

(102) Han, L.; Liu, H.; Cui, P.; Peng, Z.; Zhang, S.; Yang, J. *Sci. Rep.* **2014,** *4*, 6414. doi: 10.1038/srep06414

(103) Bao, Y. F.; Feng, L. G. *Acta Phys. -Chim. Sin.* **2021,** *37*, 2008031. [包玉菲, 冯立纲. 物理化学学报, **2021,** *37*, 2008031.] doi: 10.3866/PKU.WHXB202008031

(104) Yang, S.; Li, S.; Song, L.; Lv, Y.; Duan, Z.; Li, C.; Praeg, R. F.; Gao, D.; Chen, G. *Nano Res.* **2019,** *12*, 2881. doi: 10.1007/s12274-019-2530-5

(105) Dong, J. C.; Su, M.; Briega-Martos, V.; Li, L.; Le, J. B.; Radjenovic, P.; Zhou, X. S.; Feliu, J. M.; Tian, Z. Q.; Li, J. F. *J. Am. Chem. Soc.* **2020,** *142*, 715. doi: 10.1021/jacs.9b12803

(106) Fang, B.; Feng, L. G. *Acta Phys. -Chim. Sin.* **2020,** *36*, 1905023. [方波, 冯立纲. 物理化学学报, **2020,** *36*, 1905023.] doi: 10.3866/PKU.WHXB201905023